What Really Prevents Proton Transport through Aquaporin? Charge Self-Energy versus Proton Wire Proposals

Anton Burykin and Arieh Warshel
Department of Chemistry, University of Southern California, Los Angeles, California

ABSTRACT The nature of the control of water/proton selectivity in biological channels is a problem of a fundamental importance. Most studies of this issue have proposed that an interference with the orientational requirements of the so-called *proton wire* is the source of selectivity. The elucidation of the structures of aquaporins, which have evolved to prevent proton transfer (PT), provided a clear benchmark for exploring the selectivity problem. Previous simulations of this system have not examined, however, the actual issue of PT, but only considered the much simpler task of the transfer of water molecules. Here we take aquaporin as a benchmark and quantify the origin of the water/proton selectivity in this and related systems. This is done by evaluating in a consistent way the free energy profile for transferring a proton along the channel and relating this profile to the relevant PT rate constants. It is found that the water/proton selectivity is controlled by the change in solvation free energy upon moving the charged proton from water to the channel. The reason for the focus on the elegant concept of the proton wire and the related Grotthuss-type mechanism is also considered. It is concluded that these mechanisms are clearly important in cases with flat free energy surfaces (e.g., in bulk water, in gas phase water chains, and in infinitely long channels). However, in cases of biological channels, the actual PT mechanism is much less important than the energetics of transferring the proton charge from water to different regions in the channels.

INTRODUCTION

The nature of the proton translocation (PTR) in biological molecules has been a problem of special interest in biochemistry in general and bioenergetics in particular (Mitchell, 1961; Gennis, 1989; Okamura and Feher, 1992; Ermler et al., 1994; Wikstrom, 1998; Decoursey, 2003). Molecular understanding of this issue is crucial for the elucidation of the action of ATPase (Girvin et al., 1998), bacteriorhodopsin (Luecke et al., 1999; Luecke, 2000; Royant et al., 2000; Sass et al., 2000), cytochrome-c oxidase (Ostermeier et al., 1997; Yoshikawa et al., 1998), and other important systems.

Considerations of the molecular details of PTR processes have been quite challenging, and the main conceptual views could be roughly divided into two classes. Nagle and co-workers (Nagle and Morowitz, 1978, Nagle and Mille, 1981) proposed a model of PTR along proton wires, where the key control is provided by the orientation of the elements that constitute the wire. This view is consistent with the description of proton transfer (PT) in water and ice, where all the sites are equivalent. Recent interest (Schmitt and Voth, 1998; Vuilleumier and Borgis, 1999) in the identification of the exact mechanism of H^+ diffusion in water (the so-called Grotthuss mechanism—see Eigen, 1964; Zundel and Frish, 1986; Agmon, 1995) has probably strengthened the focus on the proton wire concept, although the issue of the reorganization of the environment has also been considered. An orthogonal point of view has been put forward by Warshel and co-workers (Warshel, 1979, 1986; Sham et al., 1999), where the key factor that controls PT in proteins in general, and PTR in particular, has been identified as the electrostatic free energy of the transferred charge. These workers were well aware of the role of the reorganization of the environment in the PT process (Warshel, 1982; Aqvist and Warshel, 1993). However, it was concluded that these effects and the reorganization of the proton donor and acceptor are of secondary importance relative to the change in solvation free energy along the proton transport path. Interestingly, theoretical studies of PTR in bacterial reaction centers and cytochrome-c oxidase (Okamura and Feher, 1992; Lancaster et al., 1996; Kannt et al., 1998) have implicitly recognized the importance of electrostatic effects by focusing on the pK_a values of ionizable groups and/or internal water molecules (Sham et al., 1999). In other words, these studies have focused on the energetics of the transferred proton as a key aspect of the PTR process. However, this was done, with the exception of Sham et al. (1999), without addressing the barrier for the PT steps or the possibility that proton charge is shared by more than one water molecule.

The emergence of structural information about proton conduction pathways in general (Okamura and Feher, 1992; Ermler et al., 1994; Ostermeier et al., 1997; Yoshikawa et al., 1998; Luecke, 2000; Royant et al., 2000) and in aquaporins in particular (Fu et al., 2000; Sui et al., 2001) led to elegant simulations studies (de Groot and Grubmüller, 2001; Kong and Ma, 2001; Tajkhorshid et al., 2002) that focused on the study of water transport, which is much simpler than the simulations of PTR. These studies, as well as studies of model systems (Pomès and Roux, 1998), or PT in the center of gramicidin (Pomès and Roux, 2002; see also discussion on the corresponding problems in Concluding Remarks),

Submitted August 1, 2003, and accepted for publication September 26, 2003.

Address reprint requests to Arieh Warshel, Tel.: 213-740-4114; Fax: 213-740-2701; E-mail: warshel@usc.edu.

0006-3495/03/12/3696/11 $2.00

concluded that the channel controls the PTR by interfering with the perfect orientation of the proton wire. Similar conclusions were also drawn by others (Murata et al., 2000; Berendsen, 2001; Sansom and Law, 2001).

Some workers (e.g., Fu et al., 2000; Sansom and Law, 2001) have pointed out that PT in aquaporin involves the loss of hydrogen-bond stabilization, but no attempt had been made to quantify this effect. In contrast to most of the above studies, an explicit study of PT in reaction centers (Sham et al., 1999) indicated that the PT is controlled by the electrostatic free energy barriers along the proton conduction chain.

One of the best ways to resolve the above controversy is to examine the origin of the proton/water selectivity in aquaporins. These proteins form transmembrane channels in cell membranes of all life forms, which are responsible for efficient permeation of water (water conductance rate close to 10^9 s^{-1}) while excluding protons. This selectivity is of crucial importance to preserving the electrochemical potential across the cell. The elucidation of the x-ray structure of aquaporins (e.g., see Sui et al., 2001) provides an excellent opportunity to explore the nature of PT in biological channels in general and the origin of proton/water selectivity in particular. In fact these systems were subjected recently to extensive simulations of water transport and the results of the simulations were interpreted in terms of a so-called *global orientational tuning* (or *proton-wire breaking*) mechanism of the water/proton selectivity (see de Groot and Grubmüller, 2001; Tajkhorshid et al., 2002). Although this is an interesting proposal it lacked one key element, namely a proper theoretical verification. That is, up to now all simulations of permeation events in aquaporin channel were done only for water molecules rather than for protons and no simulation of an actual PT was reported. Obviously, it is hard to reach any conclusion about the origin of the water/proton selectivity without exploring the transport of both water and protons. For example, as will be discussed below, the free energy associated with moving a proton to a given site is expected to be very different than that associated with the transport of a water molecule to the same site. Similarly, the fluctuations of the protein dipoles are expected to have a very different effect on a PT process and on the motion of neutral water molecules.

The progress in computer simulations of PT and related processes in solutions and proteins (Warshel, 1982, 1991; Hammes-Schiffer, 1996; Hwang and Warshel, 1996; Schmitt and Voth, 1998; Vuilleumier and Borgis, 1998; Alhambra et al., 2000; Feierberg et al., 2000; Billeter et al., 2001) has offered a practical way for microscopic studies of PTR in biological systems. In particular, the ability to simulate the promoting fluctuations (Warshel, 1982, 1991) and relate them to the relevant activation barriers by using a modified Marcus relationship (Warshel, 1984b, 1991; Aqvist and Warshel, 1993) has provided a reasonable starting point for analyzing the water/proton selectivity problem. Here we exploit this progress, using a combination of the modified Marcus expression (Hwang et al., 1988; Aqvist and Warshel, 1993) and the PDLD/S-LRA method to explore the nature of water/proton selectivity in water channels. As a benchmark, we consider the aquaporin channel AQP1, with the highest current atomic resolution (2.2 Å for the PDB entry 1J4N, see Sui et al., 2001). Although all aquaporin channels are tetramers, it is known that each monomer itself also can be functional. Thus we use only a single monomer in our simulations (see Fig. 1). Our simulations show that the H^+ transport is controlled by solvation and other electrostatic effects, basically in the same way that the transport of other ions is controlled in ion channels. The Methods section presents our theoretical approaches for modeling PT in biological channels. Results and Discussion focuses on the calculations of the energetics of H^+ conductance through the aquaporin channel. The calculations establish the existence of a very large barrier, due to the loss of solvation energy upon transfer of a proton from water to the channel interior. The Concluding Remarks section discusses the general implications of our findings in terms of the factors that control water/proton selectivity in biological systems.

METHODS

As discussed above, any question about the proton/water selectivity should be explored by performing actual calculations on both the water and proton systems. Molecular dynamics (MD) simulations were effective in modeling water transfer through the aquaporins (de Groot and Grubmüller, 2001; Tajkhorshid et al., 2002), since the barrier for such a transfer is very low. Unfortunately, the more challenging case of a PTR process cannot be explored at present by direct MD simulations since, in this case, we are dealing with a high barrier and a very long penetration time (see below).

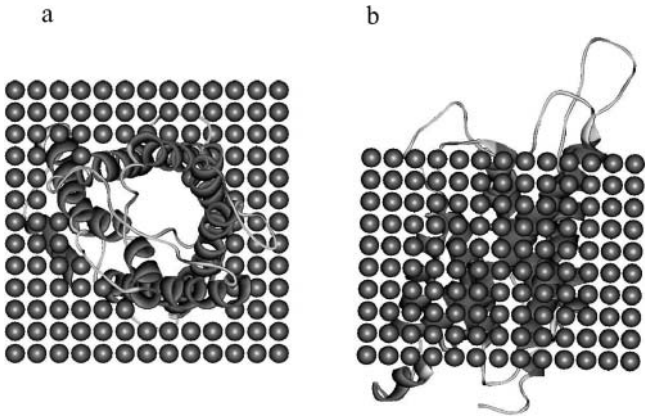

FIGURE 1 The setup of the simulation system. The aquaporin monomer is embedded in a grid of 30 × 20 × 20 Å size and 2.5 Å spacing of carbon atoms that represent the low dielectric aspects of the membrane. The figure only depicts the main chain fold of the protein and displays the system from two views (*a*, parallel, and *b*, perpendicular to the channel axis). In the actual PDLD/S-LRA simulations we consider an explicit simulation sphere, centered around the specific H_3O^+ system studied, and embedded in a water sphere subjected to the SCAAS boundary conditions (see text).

The selectivity issue in aquaporins and related systems should be resolved by a model that accurately represents the energetics of PTR in proteins. This can be done in principle by using a combined quantum mechanics/molecular mechanics molecular orbital approach (for review, see Warshel, 2003). However, at present we believe that the most effective conceptual and computational approach is provided by the empirical valence bond (EVB) model (Warshel and Weiss, 1980; Warshel, 1991; Aqvist and Warshel, 1993; Hwang and Warshel, 1996; Schmitt and Voth, 1998; Vuilleumier and Borgis, 1998) that has been used before in simulations of PT in enzymes (Warshel, 1991; Aqvist and Warshel, 1993; Hwang and Warshel, 1996), in solution (Schmitt and Voth, 1998; Vuilleumier and Borgis, 1998), and in nanotubes (Dellago et al., 2003). Although we will not use here the explicit EVB formulation we will discuss this approach to establish a rigorous base to our modeling approach.

The EVB method describes the potential energy surface and charge distribution of the quantum system embedded in a specific environment (e.g., protein) in terms of diabatic states with the proton attached to different protonation sites. These sites are then mixed by the appropriate off-diagonal terms. Here we consider, for simplicity, a quantum system of two water molecules and one proton embedded in a given environment. This system can be described by considering two states:

$$\psi_1 = (H-\overset{H}{\overset{|}{O}}_{\mathrm{a}}-H)^{+}\quad(\overset{H}{\overset{|}{O}}_{\mathrm{b}}-H)$$

$$\psi_2 = (H-\overset{H}{\overset{|}{O}}_{\mathrm{a}})\quad(H-\overset{H}{\overset{|}{O}}_{\mathrm{b}}-H)^{+}. \tag{1}$$

The energies of these states in their specific environments are described (e.g., Aqvist and Warshel, 1993) as

$$H_{11} = \varepsilon_1 = \varepsilon_{\mathrm{S}}^{(1)} + U_{\mathrm{sS}}^{(1)} + U_{\mathrm{ss}},$$
$$H_{22} = \varepsilon_2 = \varepsilon_{\mathrm{S}}^{(2)} + U_{\mathrm{sS}}^{(2)} + U_{\mathrm{ss}}, \tag{2}$$

where S and s designate, respectively, the quantum system (the *solute*) and its surrounding (the *solvent*). $\varepsilon_{\mathrm{s}}^{(\mathrm{i})}$ is described by Morse potentials, a bond-angle term, and a nonbond interaction term, which describe the interactions between the solute atoms in the i^{th} state and the solvent molecules, while U_{ss} is the solvent-solvent force field. Now, the ground state potential surface is obtained by solving the secular equation

$$\mathbf{HC}_{\mathrm{g}} = E_{\mathrm{g}}\mathbf{C}_{\mathrm{g}}. \tag{3}$$

In the simple two-states case, we have

$$E_{\mathrm{g}} = \frac{1}{2}\left[(\varepsilon_1+\varepsilon_2) - \sqrt{(\varepsilon_1-\varepsilon_2)^2 + 4H_{12}}\right]. \tag{4}$$

In cases with more states (e.g., three water molecules) we have to solve a multistate Hamiltonian, as was done repeatedly in EVB treatment (e.g., Warshel and Weiss, 1980; Warshel, 1991; Schmitt and Voth, 1998; Vuilleumier and Borgis, 1998). The solution of Eq. 3 provides the eigenvector, $\mathbf{C}_{\mathrm{g}}$, and the corresponding charge distribution. This distribution may correspond to a localized picture when the proton charge is localized on one water molecule, or to the case when the proton charge is delocalized (see Discussion). The EVB/umbrella sampling procedure (e.g., Warshel, 1991) allows one to obtain the rigorous profile of the free energy function $\Delta\bar{g}$, which corresponds to E_{g} and the free energy functions Δg_1 and Δg_2, which themselves correspond to ε_1 and ε_2, respectively (see Fig. 2). It is important to point out here that such profiles have been evaluated quantitatively in many EVB simulations of PT in proteins (for reviews see Aqvist and Warshel, 1993; Warshel, 2003). The corresponding profiles provide the activation free energy $\Delta g^{\neq}$ for the given PT step. The calculated activation barrier can then be converted to rate constant using transition state theory (e.g., see Warshel, 1991) as

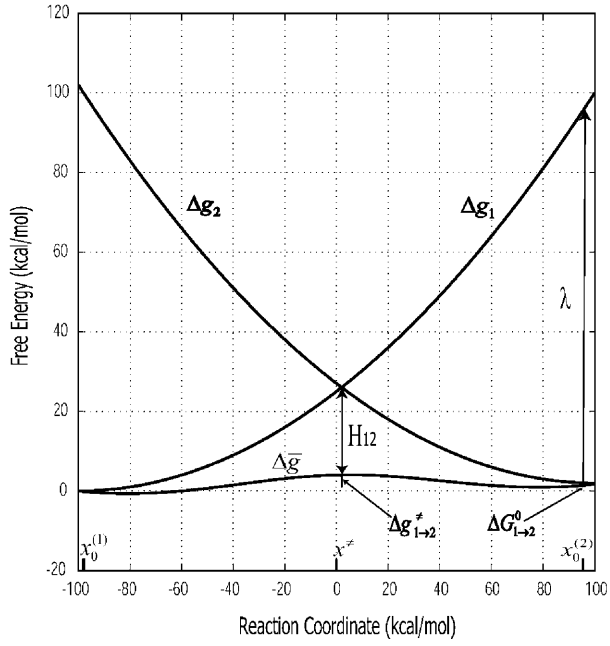

FIGURE 2 The relationship between the energetics of the valence bond states of Eq. 1 and the activation barrier of the corresponding PT process. The figure describes the results of an EVB calculation of a proton transfer between two water molecules in aquaporin. The free energy functions Δg_1 and Δg_2 of the zero-order diabatic states are converted to the ground state free energy function (ΔG) by using the EVB off-diagonal element, H_{12}. The figure defines the reorganization energy, λ; the adiabatic activation barriers, $\Delta g^{\neq}_{1\rightarrow 2}$; and the reaction free energy, $\Delta G^{0}_{1\rightarrow 2}$. The reaction coordinate is defined in terms of the energy gap between state 1 and state 2. For details, see Hwang et al. (1988).

$$k_{\mathrm{i}\rightarrow\mathrm{j}} \cong (RT/h)\exp\{-\Delta g^{\neq}_{\mathrm{i}\rightarrow\mathrm{j}}/RT\}. \tag{5}$$

A more rigorous expression for $k_{\mathrm{i}\rightarrow\mathrm{j}}$ can be obtained by multiplying the current expression by a transmission factor that can be calculated easily by running downhill trajectories (Warshel, 1991). However, the corresponding correction is usually small (Villa and Warshel, 2001) and will not change the conclusions of the present work. At any case, the calculated rate constant can now be used in calculations of proton transport process.

At this point it is useful to consider the approximated expression for $\Delta\bar{g}$ and $\Delta g^{\neq}$. Here we note that with the simple two-state model of Eq. 1 we can obtain a very useful approximation to the $\Delta\bar{g}$ curve. That is, using the above-mentioned free energy perturbation/umbrella sampling formulation, we obtain the $\Delta\bar{g}$ that corresponds to the E_{g} and the free energy functions Δg_{i} that correspond to the ε_{i} surfaces. This leads to the approximated expression

$$\Delta\bar{g}(x) = \frac{1}{2}\left[(\Delta g_1(x)+\Delta g_2(x)) - \sqrt{(\Delta g_1(x)-\Delta g_2(x))^2 + 4H_{12}(x)}\right], \tag{6}$$

where x is the generalized reaction coordinate, which is given by ε_1–ε_2. Now we can exploit the fact that the Δg_{i} curves can be approximated by parabolas of equal curvatures (this approximated relationship was found to be valid by

many microscopic simulations (e.g., Aqvist and Warshel, 1993). This approximation can be expressed as

$$\Delta g_{\mathrm{i}}(x) = \lambda \left(\frac{x - x_{\mathrm{o}}^{(\mathrm{i})}}{x_{\mathrm{o}}^{(\mathrm{j})} - x_{\mathrm{o}}^{(\mathrm{i})}} \right)^2, \tag{7}$$

where λ is the so-called *solvent reorganization energy* (which is illustrated in Fig. 2), and it is divided here into the internal contribution of the donor and acceptor, λ_{int}, and the contribution of the surrounding (the solvent), λ_{sol}.

Using Eqs. 6 and 7 or the equivalent graphical representation of Eq. 2, one obtains our modified Marcus relationship (Hwang et al., 1988; Warshel, 1991; Aqvist and Warshel, 1993),

$$\begin{aligned} \Delta g_{\mathrm{i}\to\mathrm{j}}^{\neq} &= (\Delta G_{\mathrm{i}\to\mathrm{j}}^{0} + \lambda)^2/4\lambda - H_{\mathrm{ij}}(x^{\neq}) \\ &\quad + H_{\mathrm{ij}}^2(x_0^{(\mathrm{i})})/(\Delta G_{\mathrm{i}\to\mathrm{j}}^{0} + \lambda), \\ \lambda &= \lambda_{\mathrm{int}} + \lambda_{\mathrm{sol}}, \end{aligned} \tag{8}$$

where $\Delta G_{\mathrm{i}\to\mathrm{j}}^{0}$ is the free energy of the reaction, and H_{ij} is the off-diagonal term that mixes the two relevant states whose average value at the transition state, $x^{\neq}$, and at the reactant state, $x_0^{(\mathrm{i})}$. The first term in this expression is the regular Marcus equation (Marcus, 1964), which corresponds to the intersection of Δg_1 and Δg_2 at $x^{\neq}$. The second and third terms represent, respectively, the effect of H_{12} at $x^{\neq}$ and $x_0^{(\mathrm{i})}$.

Repeated quantitative EVB studies of reactions in solutions and proteins (e.g., Warshel, 1984; Aqvist and Warshel, 1993) established the quantitative validity of Eq. 8. With this fact in mind we can take these equations as a quantitative correlation between $\Delta g_{\mathrm{i}\to\mathrm{j}}^{\neq}$ and ΔG^0. Basically, when the changes in ΔG^0 are small, we obtain a linear relationship between $\Delta g_{\mathrm{i}\to\mathrm{j}}^{\neq}$ and ΔG^0. More details about this linear free energy relationship and its performance in studies of chemical and biochemical problems are given elsewhere (Hwang et al., 1988; Warshel, 1991; Aqvist and Warshel, 1993; Warshel et al., 1994; Kong and Warshel, 1995; Schweins and Warshel, 1996).

As much as the present work is concerned, the main point of Eq. 8 and Fig. 2 is that $\Delta G_{\mathrm{i}\to\mathrm{j}}^{0}$, which determines the corresponding $\Delta g_{\mathrm{i}\to\mathrm{j}}^{\neq}$, is correlated with the difference between the two minima of the $\Delta\bar{g}$ profile that correspond to states *i* and *j*, respectively. This point will be used in our treatment and in the discussion of charge delocalization effects.

With the above considerations in mind, we adopt here the strategy developed in our early studies of biological PTR (Warshel, 1986; Sham et al., 1999), and combine semimacroscopic electrostatic calculations with the EVB conceptual picture. This is done by evaluating first the free energy of bringing a proton from the bulk solvent to the given site in the channel (i.e., to a water molecule) and then using a modified Marcus theory for the rate of PT between each site. The main ingredients of this approach are described below.

The key parameter in Eq. 8 is $\Delta G_{\mathrm{i}\to\mathrm{j}}^{0}$, and our task is to evaluate this parameter by converting the protein structure information to the energetics. Here we start formulating the energetics of all possible proton configurations (protons on different water molecules and/or on the protein residues) using, as in Sham et al. (1997),

$$\Delta G^{(\mathrm{m})} = \sum_{\mathrm{i}} \left\{ -2.3RTq_{\mathrm{i}}^{(\mathrm{m})}[pK_{\mathrm{int}}^{\mathrm{p}} - pH] + 1/2 \sum_{\mathrm{i}\neq\mathrm{j}} W_{\mathrm{ij}} q_{\mathrm{i}}^{(\mathrm{m})} q_{\mathrm{j}}^{(\mathrm{m})} \right\}, \tag{9}$$

where *m* designates the vector of the charge states of the given configuration—i.e., $m = (q_{\mathrm{i}}^{(\mathrm{m})}, q_2{}^{(\mathrm{m})} \ldots q_{\mathrm{n}}{}^{(\mathrm{m})})$. Here, $q_{\mathrm{i}}^{(\mathrm{m})}$ is the actual charge of the i^{th} group (e.g., hydronium ion) at the m^{th} configuration. This can be 0 or −1 for acids and 0 or 1 for bases (where we restrict our formulation to mono ions, although the extension to $|q| > 1$ is trivial). The $W_{\mathrm{ij}}q_iq_{\mathrm{j}}$ term represents the charge-charge interaction. The intrinsic pK_{a} (pK_{int}) is the pK_{a} value that the given ionizable group would have when all other ionizable groups were kept at their neutral state (the evaluation of this term is described in Sham et al., 1997).

Now, the $\Delta G^{(\mathrm{m})}$ values can be converted to the corresponding energy of protonating the different sites. This can be obtained by (Warshel, 1979),

$$\Delta G_{\mathrm{H}^+} = \sum_{\mathrm{i}} \Delta G_{\mathrm{H}^+}^{(\mathrm{m,i})} = \sum_{\mathrm{i}} (\Delta G^{(\mathrm{m})})_{\mathrm{i}} q_{\mathrm{i}}^{\mathrm{m}}, \tag{10}$$

where ΔG_{H^+} is the free energy of the given proton configuration, and $(\Delta G^{(\mathrm{m})})_{\mathrm{i}}$ is the contribution to Eq. 9 from its i^{th} term. In more explicit form, we can write

$$\begin{aligned} \Delta\Delta G_{\mathrm{H}^+}^{(\mathrm{m,i})}(B_{\mathrm{i}} \to B_{\mathrm{i}}H^+) &= -2.3RT[pK_{\mathrm{a}}^{\mathrm{w}}(B_{\mathrm{i}}H^+) - pH] \\ &\quad + (\Delta\Delta G_{\mathrm{sol}}^{\mathrm{w}\to\mathrm{p}}(q_{\mathrm{i}}^{(\mathrm{m})}))_0 \\ &\quad + \sum_{\mathrm{j}\neq 1} W_{\mathrm{ij}} q_{\mathrm{i}}^{(\mathrm{m})} q_{\mathrm{j}}^{(\mathrm{m})}, \end{aligned} \tag{11}$$

where B_{i} designates the i^{th} base, and $\Delta\Delta G_{\mathrm{sol}}^{\mathrm{w}\to\mathrm{p}}$ designates the change in the solvation free energy of BH^+ upon transfer from water to the specific protein site.

The key parameters in Eqs. 7–9 are the change in solvation free energies: $\Delta G_{\mathrm{sol}}^{\mathrm{w}\to\mathrm{p}}(q_{\mathrm{i}}^{(\mathrm{m})})$, which are thus also the key parameters in Eq. 8. The calculations of these parameters are accomplished by using the semimicroscopic version of the protein-dipoles-Langevin-dipoles (PDLD/S) method (Lee et al., 1993; Sham et al., 1997). The effect of the protein reorganization is considered explicitly in these calculations by using the linear response approximation (LRA) and evaluating the PDLD/S energies for the charged and uncharged states of the relevant residues. For more details of the PDLD/S-LRA method, see Lee et al. (1993) and Sham et al. (1997). The charge-charge interaction term W_{ij} can be calculated in an explicit way (see Lee et al., 1993; Sham et al., 1997). However, in most cases, we obtain good results by using

$$W_{\mathrm{ij}} = 332/(r_{\mathrm{ij}}\varepsilon_{\mathrm{ij}}), \tag{12}$$

where r_{ij} is the distance between the interacting groups, and $\varepsilon_{\mathrm{ij}}$ is an effective dielectric constant whose value is determined by a distance-dependent function (Warshel and Russell, 1984; Lee et al., 1993). The justification of this approximation is discussed in detail elsewhere (Lee et al., 1993; Sham et al., 1997; Schutz and Warshel, 2001). Basically, ε for charge-charge interaction reflects the compensation of the gas phase Coulomb interaction between the charges by the solvation effect of the protein plus solvent system. This compensation has been found to be unexpectedly large even for charge-charge interaction in the protein interior, leading to a large effective $\varepsilon_{\mathrm{ij}}$ (between 20 and 40). This fact has been established repeatedly by both theoretical and experimental studies (e.g., Sham et al., 1998; Johnson and Parson, 2002). It is also important to realize that $\varepsilon_{\mathrm{ij}}$ is not equal to, but is typically much larger than, the dielectric constant ε_{p} that determines $\Delta\Delta G_{\mathrm{sol}}^{\mathrm{w}\to\mathrm{p}}$ (see Schutz and Warshel, 2001; and Discussion below).

The PDLD/S-LRA calculations considered the free energy profile for transfer of an H_3O^+ (or a water molecule) to any position along the channel axis (any value of *z*-coordinate). This study involved two levels of calculations. In the first step we performed explicit all-atom MD simulations with the surface-constrained all-atom solvent (SCAAS) (King and Warshel, 1989) and the local reaction field (LRF) long-range treatment (Lee and Warshel, 1992) to generate protein configurations with the charged and uncharged forms of the solute. In the next step we performed the PDLD/S calculations on the generated configuration and took their average as the consistent estimate of the self-energy. These two sets of calculations involved two different simulation systems and different boundary conditions. The first system is an all-atom system constructed by embedding the protein in a membrane (Fig. 1). The explicit part of the simulation system was constructed by taking the H_3O^+ ion (or water molecule) under consideration, constraining its position to a given *z*-value and then constructing an SCAAS simulation sphere around this ion, including in the system (in addition to the centered ion) the protein and membrane atoms

as well as the water molecules within 24 Å from the center. The membrane was represented by a cubic grid of induced dipoles with a 2.5 Å spacing and a polarizability of 1.3 Å^3, determined from the Clausius-Mossotti equation. This type of treatment, which has been used before in our studies (e.g., Aqvist and Warshel, 1989; Burykin et al., 2002, 2003), provides reliable results for the most important features of the membrane (i.e., its effect as a low dielectric region). Long-range effects were treated by the LRF approach. The all-atom simulations were used to generate 10 configurations for the charged and uncharged states. Each of these simulations was run for 2 ps at 300 K, starting from the previous configurations.

The configurations generated by the all-atom simulations were used in the PDLD/S-LRA calculations. This simulation system involved a spherical system of a radius of 24 Å around the specific position of the hydronium ion (or the water molecule) under study, and an LRF long-range treatment. The rest of the protein/membrane system is then described as a continuum with $\varepsilon = 80$. The detailed constructions of such simulation systems are described extensively elsewhere (e.g., Lee et al., 1993), including discussion and demonstration of the validity of our long-range and boundary conditions and treatment (e.g., Alden et al., 1995). The protein was treated with $\varepsilon_p = 4$ and the contribution of the membrane region was evaluated by treating the membrane as a part of the protein with a dielectric constant of $\varepsilon_m = \varepsilon_p = 4$. The use of a membrane dielectric of 4 (rather than 2) reflected the possibility that the membrane/protein interface contains water molecules (see Alden et al., 1995). The possible effect of changing the membrane dielectric to 2 can be estimated in specific cases by considering the energetics of the induced dipoles on the membrane (using the iterative approach of Warshel and Levitt, 1976) and evaluating the microscopic effect of changing ε_m from 4 to 2. The PDLD/S sphere was surrounded by a continuum with $\varepsilon = \varepsilon_w$. The PDLD/S calculations were averaged over the above-mentioned configurations of the charged and uncharged states, as required by the LRA procedure.

All the self-energy calculations were done with the program MOLARIS, which combines the ENZYMIX and POLARIS programs (Lee et al., 1993). The MD simulations (needed to generate the protein configurations) were performed by the ENZYMIX module with the parameter set of Lee et al. (1993), which included the effect of the induced dipoles. The force field parameters of H_3O^+ and H_2O are given in Table 1 (see also Fig. 3).

The actual free energy of H_3O^+ in the i^{th} site should also reflect the effect of the ionizable groups of the protein. This contribution was evaluated by the W_{ij} term of Eqs. 11 and 12.

The ionization states of the protein groups at pH = 7.0 were evaluated by calculating the corresponding apparent pK_a values. These calculations were started by using the PDLD/S-LRA to find the intrinsic pK_a of each ionized residue and then using a self-consistent hybrid approach (see Sham et al., 1997), with the charge-charge interaction term of Eq. 12 for the interaction between the ionized residues, to determine their apparent pK_a values.

After obtaining the solvation profile we should convert it to the actual free energy profile $\Delta\bar{g}$. This is done by using Eq. 6 for each PT step. In so-doing, we keep the donor-acceptor distance at an optimal value of 2.8 Å and 2.5 Å for the ground state and the transition state, respectively. This treatment is based on the finding that when the actual distance is larger the work of moving to the optimal distance is rather small (Sham et al., 1999). For the 2.8 Å and 2.5 Å separation distance we used H_{12} values of 20 kcal/mol and 10 kcal/mol, respectively, in agreement with the corresponding average values from EVB simulations. The value of λ was taken as 85 kcal/mol, representing a typical value from simulations inside the channel (see Fig. 2).

TABLE 1 H_3O^+ and H_2O classical force field parameters (see also Fig. 3)

Bond parameters	K (kcal × mol^{-1} × Å^{-2})	r_0 (Å)
O_W–H_W	239.0	0.998
O_H–H_H	239.0	0.998
Angle parameters	**K (kcal × mol^{-1} × degree^{-2})**	**θ_0 (degree)**
H_W–O_W–H_W	70.0	106.5
H_H–O_H–H_H	70.0	112.0
Atom	**Charge (a.u.)**	
O_W	−0.80	
H_W	0.40	
O_H	−0.65	
H_H	0.55	
Van der Waals	**A (kcal × mol^{-1} × Å^6)**	**B (kcal × mol^{-1} × Å^3)**
O_W	774.0	24.0
H_W	0.12	0.0
O_H	220.0	24.0
H_H	4.0	0.0

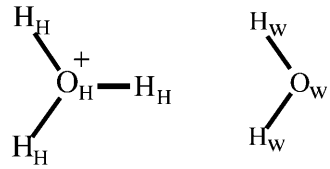

FIGURE 3 Assignment of atom types for H_3O^+ and H_2O in the classical MD simulations used to generate configurations for the PDLD/S-LRA calculations.

RESULTS AND DISCUSSION

The PDLD/S-LRA free energy profiles for the transfer of H_3O^+ and H_2O through the aquaporin water channel are depicted in Fig. 4. The profile reflects all the electrostatics contributions of the protein except the effect of the ionized residues. Thus Fig. 5 reflects the desolvation penalty and the ''back field'' from the protein permanent dipoles including the so-called helix dipoles (note, however, that the effect of the helix macrodipoles contributes much less that is usually

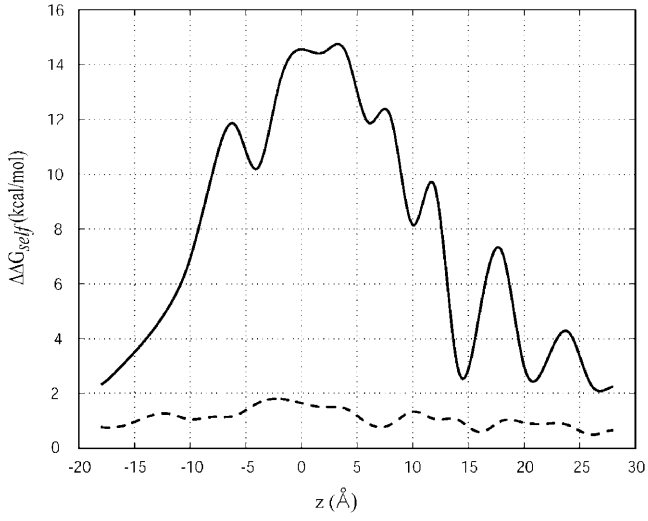

FIGURE 4 The PDLD/S-LRA free energy profile for H_3O^+ (—) and H_2O (- - -) transfer through the aquaporin water channel/membrane system, where the channel ionizable groups are kept in their neutral form. $\Delta\Delta G_{self}$ corresponds here to the $\Delta\Delta G_{sol}$ of Eq. 11.

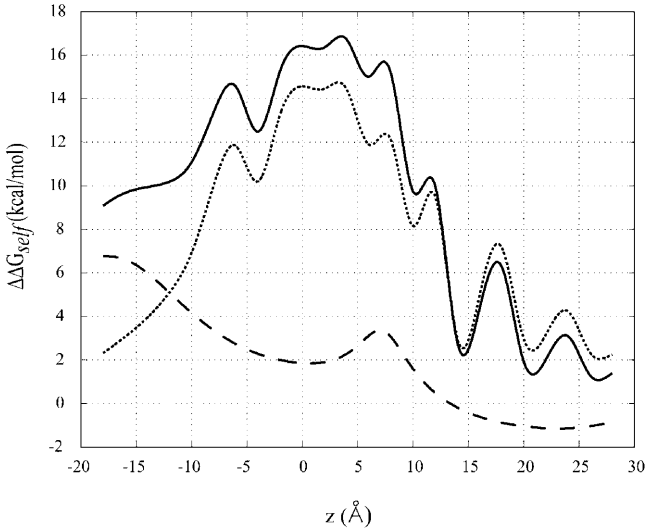

FIGURE 5 The free energy profile for H_3O^+ transfer in aquaporin both with (*solid line*) and without (*dotted line*) the effect of the ionizable residues. The separate contribution of the ionized residues (*dashed line*) is also shown. $\Delta\Delta G_{self}$ includes here both $\Delta\Delta G_{sol}$ and the charge-charge interaction term.

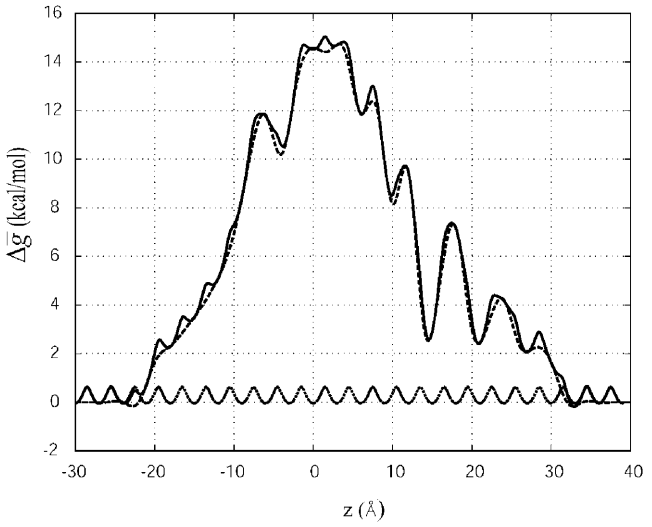

FIGURE 6 Illustrating the relative importance of the chemical barrier for water-water proton jump and the electrostatic barrier for water-membrane charge transfer. The figure shows the free energy profile $\Delta\bar{g}$ (*solid line*) with the free energy barriers associated with the proton jumps, and the electrostatic profile without the proton jumps contribution (*dashed line*). The separated proton jumps contributions are also shown (*dotted line*). For simplicity, we considered the electrostatic profile without the effect of the ionizable groups. Furthermore, the EVB-type chemical profiles were obtained with the same parameters for each jump.

assumed and its main effect is due to the localized microscopic dipoles at the end of the helix; see, e.g., Aqvist et al., 1991; Burykin et al., 2003). At any rate, as seen from the figure the barrier heights for H_3O^+ and H_2O are ~15.0 kcal/mol and 1.8 kcal/mol, respectively. This corresponds to permeation times of 10^{-11}s and 10^{-2}s for the water and proton, respectively (thus the ratio of the penetration times is $\sim 10^9$). This extremely large penetration time makes it impossible for protons to go through the aquaporin channel during reasonable physiological times.

Since the above study was done while considering only the solvation energy term, it is important to examine the effect of the protein-ionized groups at pH = 7. This effect was examined using Eq. 12 with $\varepsilon_{ij} = 30$ and the corresponding results are given in Fig. 5. Similar results were obtained with the distance-dependent function of Schutz and Warshel (2001). As seen from the figure we obtain basically the same trend as in Fig. 4. This indicates that the main factor that controls the proton transport is the solvation energy term (see also below).

Our PDLD/S-LRA calculations did not consider the chemical effect of proton transfer between neighboring water molecules, which might, in principle, give a different picture. Thus we used Eq. 6 and converted the electrostatic profile of Fig. 4 to the corresponding EVB profile. As seen from Fig. 6, the resulting EVB profile follows basically the electrostatic profile and has the same feature of an extremely high barrier at the center of the channel. Apparently, as argued repeatedly before (Warshel, 1979, 1986; Sham et al., 1999), the key factor that controls PT in biological systems is the electrostatic barrier and not the detailed orientation of the donor and acceptor as implied by the proton-wire model (for more discussion of the issue of charge delocalization and other effects, see below, and the next section).

The proton exclusion effect has been attributed by almost all structural studies (e.g., Murata et al., 2000) and simulation studies (de Groot and Grubmüller, 2001; Kong and Ma, 2001; Tajkhorshid et al., 2002) to the break of the proton wire (single file of water molecules) in the middle of the channel due to the so-called NPA (asparagine, proline, alanine) motif. In other words, it has been concluded that the interaction of the water molecules with the elements of the NPA forces the water molecule in this region to orient in a way which is very different from the classical uniform orientation of water molecules in proton wires (which is presumably needed for an effective PTR). This reflects the assumption that the selectivity is due to ''global orientational tuning'' rather than to the dielectric barrier identified in the present work. Since the center of the channel is approximately at the region of the NPA motif, it is important to clarify that the high calculated barrier is not due to this motif. To clarify this point, we repeat our calculations for a much simpler system, namely for nonpolar membrane with a 4 Å radius pore. Such a narrow pore allows single-file water permeation (see Hummer et al., 2001) but in contrast to the aquaporin channel, this pore provides a completely homogenous environment without the NPA (or any other) motifs that could break a proton wire. Thus any calculated barrier in the system should be attributed to the difference in the dielectric environments between water and the membrane grid.

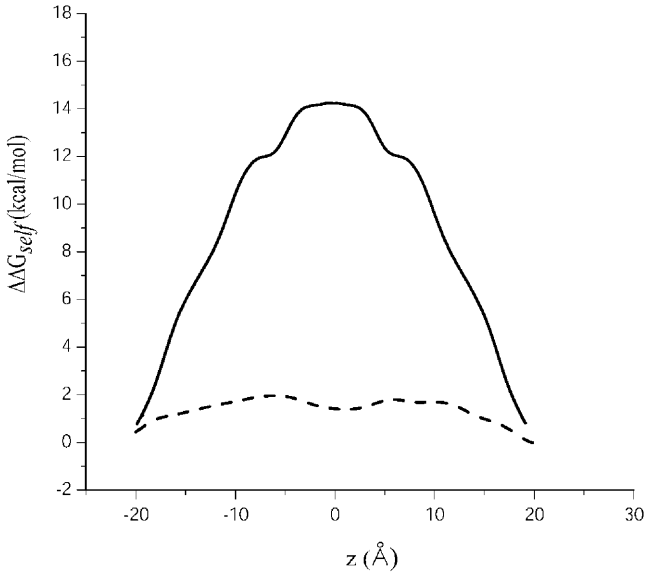

FIGURE 7 The PDLD/S-LRA free energy profile for H_3O^+ (—) and H_2O (- - -) transfer through 4 Å radius hole in the membrane. $\Delta\Delta G_{self}$ corresponds to $\Delta\Delta G_{sol}$ of Eq. 11.

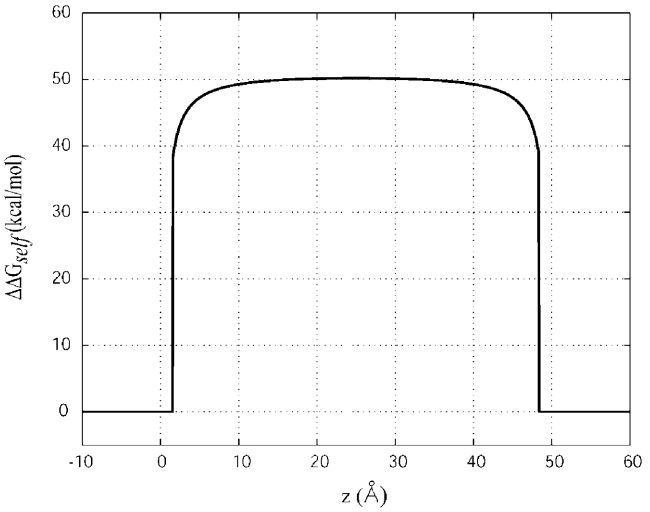

FIGURE 8 The free energy profile for transfer of a unit charge of radius $\bar{a} = 1.6$ Å through a membrane of a width $L = 50$ Å and dielectric constant $\varepsilon = 2$.

The self-energy for the proton penetration profile (Fig. 7) in the above system shows again the same trend as the corresponding profile in aquaporin, producing an enormous difference between the overall barriers for proton and water penetration. Thus we must conclude that the proton/water selectivity has purely electrostatic origin (due to the difference in solvations) and has little to do with the NPA motif or water molecule orientations. In fact, as one can see from comparison of Figs. 4 and 7, the maximum of the free energy profile corresponds simply to the center of the membrane.

The fact that a transfer of a charge through a low dielectric membrane involves a high free energy barrier can be reproduced by a simple analytical expression. That is, the free energy profile for transferring a unit charge of a radius $\bar{a}$ through a membrane (with dielectric constant ε') of a width L is given by Warshel (1981), and Warshel et al. (1984); see also Parsegian (1969) and Kitzing and Soumpasis (1996) for the related treatment, as

$$\Delta G_{sol}(Z) \approx 166\left[\frac{1}{2\bar{a}} - \left[\frac{1}{8Z} + \frac{1}{8(L-Z)}\right]\right], \qquad (13)$$

where the energy is given in kcal/mol, while $\bar{a}$, L, and Z are given in Å (here we assumed that $\varepsilon' = 2$).

In this work we demonstrated that the free energy profile for the PTR process follows the ΔGs profile. With this in mind we can estimate the effective H_3O^+ radius $\bar{a}$ using the Born's formula, $\Delta G^{w}_{sol} = -166(q^2/\bar{a})(1 - 1/\varepsilon_w)$, where ΔG is solvation free energy of H_3O^+ in water. Using the experimental values of $\Delta G^{w}_{sol} = -105$ kcal/mol and $\varepsilon_w = 80$, we obtain $\bar{a} = 1.6$ Å. The free energy profile for $\bar{a}$=1.6 Å and membrane length of $L = 50$ Å is shown in Fig. 8. As seen from the figure this profile has the same shape as our numerical PDLD/S results and it was obtained only from consideration of regions with different dielectric constants. In fact, the upper limit of the electrostatic barrier can be estimated by thinking about a transfer of a unit charge of a radius $\bar{a}$ from water to an infinite membrane with $\varepsilon = \varepsilon'$, which gives

$$\Delta\Delta G_{sol}(\varepsilon = 80 \rightarrow \varepsilon = \varepsilon') = 166\frac{q^2}{\bar{a}}\left[\left(1 - \frac{1}{\varepsilon'}\right) - \left(1 - \frac{1}{80}\right)\right] \approx 166\frac{q^2}{\bar{a}\varepsilon'}. \qquad (14)$$

For $\bar{a} = 1.6\,\mathring{A}$ and $\varepsilon' = 2$ we get $\Delta G_{sol} \sim 50$ kcal/mol. However, the aquaporin channel is not a fully nonpolar medium since it includes water molecules and some polar protein residues, and the PDLD/S-LRA barrier ($\Delta G_{sol} \approx 15$ kcal/mol) is reproduced with $\varepsilon' \approx 7$.

The great impact of studies of the Grotthuss and related mechanisms might make one wonder whether we took these important effects into consideration. Here it is useful to point out that one of us has perhaps been the first to model realistic PT processes in solutions and proteins (Warshel, 1982, 1984a), and thus we are obviously well aware of the role of the reorganization of the environment. However, as is shown by the EVB calculations of Fig. 2, which have been established as a powerful tool of exploring and simulating Grotthuss-type effects (e.g., Schmitt and Voth, 1998; Vuilleumier and Borgis, 1999), the barrier for a single step PT is extremely small (~1.0 kcal/mol compared to the overall 15.0 kcal/mol barrier). Furthermore, EVB simulations of concerted PT that involved three water molecules gave again a very small barrier as long as the ΔG^0_{ij} was small. Thus, although the difference between various Grotthuss-

type mechanisms is of great interest in bulk water (where we have a competition between different processes with very low barriers), in the case of aquaporin and other channels, the physics is determined by one large barrier (the electrostatic barrier).

CONCLUDING REMARKS

The elucidation of the structure of aquaporins provided an excellent opportunity to explore the nature of biological PTR. These systems allow almost perfect transfer of water molecules but prevent the transfer of protons. This proton/water selectivity has been attributed to special orientational effects that were thought to destroy the perfect proton wire arrangement (Murata et al., 2000; Berendsen, 2001; de Groot and Grubmüller, 2001; Kong and Ma, 2001; Sansom and Law, 2001; Zeuthen, 2001; Law and Sansom, 2002; Tajkhorshid et al., 2002). The present work demonstrated that the proton selectivity reflects mainly the electrostatic barrier for transferring a charge through a low dielectric region. Thus the most important factor that controls the PTR is not much different than the factors that control regular ion transport.

The present study explored the profile for PTR not only in aquaporin but also in a hypothetical nonpolar channel (Fig. 7). This study is directly related to the issue of proton conduction through carbon nanotubes. This problem has attracted significant current interest (e.g., Dellago et al., 2003) but we are not aware of any study of the relevant free energy profile. Our calculations predict that narrow nanotubes will prevent proton conductance and thus provide large proton selectivity.

The present work considered a PTR pathway that only included water molecules as proton acceptor. A more complete treatment should include protein residues with the appropriate $p\mathrm{K_a}$ values. Such a treatment, which was already reported in our previous study (Sham et al., 1999), will lead to additional features in the PTR profile, but this will not eliminate any of the high barriers obtained in this study.

Studies of PT of an excess proton in water (Schmitt and Voth, 1998; Vuilleumier and Borgis, 1999) have used the EVB model in quantitative studies that focused on the difference between such processes as the Grotthuss and related mechanisms (Eigen, 1964; Zundel and Frish, 1986; Agmon, 1995). Significant effort was also invested in determining the role of quantum mechanical nuclear effects. These studies dealt correctly with the electrostatic effects of the environment and the effect of the solvent reorganization (since these factors are considered automatically in the EVB treatment). However, since $\Delta G_{\mathrm{i}\rightarrow\mathrm{j}} = 0$ for any PT step in bulk water, the key role of $\Delta G^0_{\mathrm{i}\rightarrow\mathrm{j}}$ in controlling PTR in heterogeneous environments was not considered. Now, the elegance of these EVB studies and the appealing features of the concerted mechanisms have probably led many to assume that the detailed nature of the PT process is the key factor in the control of biological PTR. However, as was pointed out by one of us (Warshel, 1986; Sham et al., 1999), and as demonstrated in the present work, the most important factor is the electrostatic barrier. Of course, in a system that was optimized to promote PTR, the dielectric barrier is flattened by providing better ''solvation'' for the proton and the evaluation of the detailed barrier in each step will become important.

A possible misunderstanding of our EVB-based treatment might be associated with an oversimplified analysis of the correct finding (Pomès and Roux, 1998; Wu and Voth, 2003) that the charge distribution of the protonated water chain can, frequently, be delocalized in the form of an $H_5O_2^+$ ion, rather than localized as an H_3O^+ ion. This fact might lead some to assume that the correct electrostatic profile should have been evaluated by considering the solvation of the delocalized charge distribution of an $H_5O_2^+$ system (or even a more delocalized system), rather than the H_3O^+ system considered here. However, this perception overlooks the fact that the EVB free energy profile reflects what is perhaps the most rigorous treatment of charge delocalization effects in solutions and proteins (including nonequilibrium solvation effects; Villa and Warshel, 2001). In this treatment one first evaluates the salvation of the localized diabatic states (e.g., Eq. 1) and then mixes these states and obtains the corresponding delocalization of the adiabatic state. Of course, one may try to evaluate first the solvation of the delocalized gas phase charge distribution, and then let the solvent be polarized by this distribution, and finally recalculate the charge distribution and solvation under the effect of the polarized solvent. Unfortunately, such a self-consistent approach converges much more slowly than the EVB approach, and makes it almost impossible to evaluate nonequilibrium solvation effects. At any rate, with the physically consistent EVB type treatment we obtain the correct free energy profile, $\Delta\bar{g}$, and correct charge distribution, where for $|H_{12}| > \lambda + \Delta G^0$ we will obtain a delocalized charge distribution. In other words, our $\Delta\bar{g}$ profile at the reactant and product minima in Fig. 2 does reflect the effect of H_{12}, which can be significant at the limit when $|H_{12}| > \lambda + \Delta G^0$. However, as seen from Fig. 2, this is not the case in our system. Moreover, in the most crucial parts of the profile, when $\Delta G^0_{\mathrm{i}\rightarrow\mathrm{j}}$ starts to increase fast, one finds (using Eqs. 6 and 7 and the values of H_{12} and λ mentioned in Methods) that $\Delta g(x_{\mathrm{i}} \rightarrow x_{\mathrm{j}}) \approx \Delta G^0_{\mathrm{sol}}$. This means that the $\Delta\bar{g}$ profile follows the $\Delta G^0_{\mathrm{sol}}$ profile.

The focus on the configurations of the proton wire has probably been influenced by calculations that considered hydrogen-bonded chains in vacuum (e.g., Scheiner, 1981; Pomès and Roux, 1998). However, vacuum studies do not reflect the key factor of the transfer of the proton from a high dielectric region (water) to low dielectric regions (e.g., nonpolar sites in proteins). In a long chain in vacuum the situation is similar to that in bulk water since each site has the same energy. In a shorter chain the charge is stable only at

the center (opposite to the situation in aquaporin) and we have a minimum instead of a barrier. Similar difficulties exist with regards to the consideration of proton transport through nonpolar membranes (Marrink et al., 1996; Pomès and Roux, 1998). The problem is not so much in forming a single-file chain or in the fluctuations of this file (although this would requires significant investment of free energy). The key problem is the electrostatic effects of the nonpolar environment around the file. That is, a nonpolar surrounding means enormous investment in energy for the process of transferring a proton from water to the center of the membrane.

Attempts to correlate the reorganizational fluctuations of a single-file water chain with PT in channels (Marrink et al., 1996; Pomès and Roux, 1998) have perhaps led to some of the current concepts about the selectivity of aquaporin. However, the relevant fluctuations should have been considered by evaluating the solvent reorganization energy in the presence of an actual proton and in realistic sites of the given channel. As was shown in many of our early studies of this problem (e.g., Aqvist and Warshel, 1993) and in the present case, the correct adiabatic barrier associated with the solvent reorganization energy is quite small for small separation between the donor and acceptor (due to the effect of H_{12}) and, thus, the key factor is ΔG_0. In other words, calculations of the overall dipolar reorientation in the absence of the proton are not related directly to the energetics of the PT process, and we are not aware of any formulation that established such a relationship in a consistent way. On the other hand, the EVB provides a relatively rigorous framework that relates the protein (or solvent) dipolar reorganization to the free energy profile for the PT process. This formulation (e.g., Eqs. 6 and 8) tells us exactly what type of reorganization energy $\lambda_{i\rightarrow j}$ should be considered in any specific PT step. Here the λ-values reflect the change in the solute charge, as established by Marcus long ago (Marcus, 1964) (see also below).

Attempts to consider the actual gramicidin channel (Pomès and Roux, 2002) were also put forward as a support of the Nagle proton-wire mechanism. However, the calculations were restricted to the center of the channel and did not evaluate the energy for moving the proton from water to the channel.

In addressing the general control of PTR in the biological channel, it is important to consider the distance (R_{ij}) between the donor and acceptor water molecules. This effect comes through the strong dependence of λ_{ij} on R_{ij}. That is, the outer sphere reorganization energy λ_{sol} depends on the donor and acceptor distance (Marcus, 1964):

$$\lambda_{sol} = 166\left[\frac{1}{\bar{a}} - \frac{1}{R_{ij}}\right]. \quad (15)$$

Similarly, the EVB λ_{in} increases strongly with the increase of R_{ij}. Now using Eq. 8 with $\Delta G_0 \ll \lambda$ we find that $\Delta g^{\neq}$ increases linearly with λ and thus with R_{ij}. Similar conclusions are obtained by actual EVB calculations, where it is found that $\Delta g^{\neq}$ increases rapidly when the donor and acceptor are separated by >4.5 Å. Fortunately, in most cases the work of bringing the donor and acceptor to an optimal distance ($R_{ij} \leq 3$ Å) is trivial (see Sham et al., 1999) relative to the dielectric barrier. Thus, the actual $\Delta g^{\neq}_{ij}$ for an individual PT is small and is related to the individual ΔG^0_{ij}. Only in biological systems which were designed to create switches by separating the donor and acceptor (which can be amino acids rather than water molecules) will we have to focus on the effect of the distance between the donor and acceptor. Now, because of the large dependence on R_{ij}, we should only consider a PT between neighboring water molecules. Of course, we may examine whether a sequential transfer in a chain O_i–H_i, O_j–H_j, O_k–H_k (first transfer H_i to O_j and then transfer H_j to O_k) is slower than the concerted process, whereas H_i and H_j are transferred simultaneously. However, the difference between the concerted and stepwise mechanisms is rather trivial as compared to the electrostatic effects on ΔG^0. In this respect it might be useful to comment on the appealing idea that the proton will be conducted through the channel in the same way as an injected charge in a semiconductor (moving through a barrierless conduction-band-like system). Here, the use of the EVB and proper electrostatic considerations move us back to the same considerations introduced in our early studies of electron transport in conduction chains (Warshel, 1981; Warshel and Schlosser, 1981). A system with an electrostatic barrier does not provide the picture of conduction bands but a picture of separated localized states whose energetics and dynamics are controlled by the self-energy of each state (see Warshel and Schlosser, 1981).

It should also be pointed out here that the nature of PT in the center of the channel is still a topic of significant interest. It is clearly instructive to determine how the promoting fluctuations of the environment are coupled to the PT process (note that a large body of related studies is already provided in studies of PT in the proteins; Warshel, 1984a). Here the focus on the time-dependent EVB energy gap (Warshel, 1982, 1984a, 2002; Strajbl et al., 2002) should be particularly useful. However, the elegance of the description of PT dynamics should not obscure the key factor, which is the overall free energy barrier. Here, the main control occurs already in the initial transfer from water to the channel ($Z < -10$ Å) in Fig. 4, and the nature of the PT at the center of the channel is less important.

Note added in proof: Very recent papers of two research groups (de Groot et al., 2003; Jensen et al., 2003), which were published after the acceptance of our paper, consider electrostatic contributions to the proton selectivity of aquaporin. Both research groups consider now factors that were missing in their previous proton wire proposal. The present considerations involve some elements similar to our original assertion (e.g., Warshel, 1979; Sham et al., 1999) but they still overlook the nature of some key electrostatic effects. de Groot et al, (2003) presents free energy profiles that lead to a significant barrier at the center of the channel. However, this barrier is

attributed to the effect of helix macrodipoles near the NPA region. Our studies (see text) suggest that the effects of macrodipoles are much smaller than usually assumed. Furthermore, as shown in this work, the barrier exists even when all the protein residual charges are set to zero. Obtaining quantitative results for charge transfer by microscopic calculations is extremely challenging (e.g., see discussion in Burykin et al., 2003), and it is not clear if the interesting calculations of de Groot et al. (2003) are accurate enough, since calibration against systems with known answers is not presented. Jensen et al. (2003) suggest that the proton exclusion is still associated with the dipolar water arrangement, but argue that electrostatic interactions between the proton and the channel play a major role. However, the protein response to the probe charge is not included in that study.

We are grateful to the University of Southern California's high-performance computing center for computer time.

This work was supported by National Institutes of Health grant GM40283.

REFERENCES

Agmon, N. 1995. The Grotthuss mechanism. *Chem. Phys. Lett.* 244:456–462.

Alden, R. G., W. W. Parson, Z. T. Chu, and A. Warshel. 1995. Calculations of electrostatic energies in photosynthetic reaction centers. *J. Am. Chem. Soc.* 117:12284–12298.

Alhambra, C., J. C. Corchado, M. L. Sanchez, J. Gao, and D. G. Truhlar. 2000. Quantum dynamics of hydride transfer in enzyme catalysis. *J. Am. Chem. Soc.* 122:8197–8203.

Aqvist, J., H. Luecke, F. A. Quiocho, and A. Warshel. 1991. Dipoles localized at helix termini of proteins stabilize charges. *Proc. Natl. Acad. Sci. USA.* 88:2026–2030.

Aqvist, J., and A. Warshel. 1989. Energetics of ion permeation through membrane channels. Solvation of Na^+ by gramicidin A. *Biophys. J.* 56:171–182.

Aqvist, J., and A. Warshel. 1993. Simulation of enzyme reactions using valence bond force fields and other hybrid quantum/classical approaches. *Chem. Rev.* 93:2523–2544.

Berendsen, H. J. C. 2001. Reality simulation—observe while it happens. *Science.* 294:2304–2305.

Billeter, S. R., S. P. Webb, T. Iordanov, P. K. Agarwal, and S. Hammes-Schiffer. 2001. Hybrid approach for including electronic and nuclear quantum effects in molecular dynamics simulations of hydrogen transfer reactions in enzymes. *J. Chem. Phys.* 114:6925–6936.

Burykin, A., M. Kato, and A. Warshel. 2003. Exploring the origin of the ion selectivity of the KcsA potassium channel. *Proteins.* 52:412–426.

Burykin, A., C. N. Schutz, J. Villa, and A. Warshel. 2002. Simulations of ion current in realistic models of ion channels: the KcsA potassium channel. *Prot. Struc. Func. Gen.* 47:265–280.

de Groot, B. L., T. Frigate, V. Helms, and H. Grubmüller. 2003. The mechanism of proton exclusion in aquaporin-1 channel. *J. Mol. Biol.* 333:279–293.

de Groot, B., and H. Grubmüller. 2001. Water permeation across biological membranes: mechanism and dynamics of aquaporin-1 and GlpF. *Science.* 294:2353–2357.

Decoursey, T. E. 2003. Voltage-gated proton channels and other proton transfer pathways. *Physiol. Rev.* 83:475–579.

Dellago, C., M. Naor, and G. Hummer. 2003. Proton transport through water-filled nanotubes. *Phys. Rev. Lett.* 90:105902/1–105902/4.

Eigen, M. 1964. Proton transfer, acid-base catalysis, and enzymatic hydrolysis. *Angew. Chem. Int. Ed. Engl.* 3:1–72.

Ermler, U., G. Fritzsch, S. K. Buchanan, and H. Michel. 1994. Structure of the photosynthetic reaction centre from *Rhodobacter sphaeroides* at 2.65-E resolution: cofactors and protein-cofactor interactions. *Structure.* 2:925–936.

Feierberg, I., V. Luzhkov, and J. Eqvist. 2000. Computer simulation of primary kinetic isotope effects in the proposed rate limiting step of the glyoxalase I catalyzed reaction. *J. Biol. Chem.* 275:22657–22662.

Fu, D., A. Libson, L. Miercke, C. Weitzmann, P. Nollert, J. Krucinski, and R. M. Stroud. 2000. Structure of a glycerol conducting channel and the basis for its selectivity. *Science.* 290:481–486.

Gennis, R. B. 1989. Biomembranes: Molecular Structure and Function. Springer-Verlag, New York.

Girvin, M. E., V. K. Rastogi, F. Abildgaard, J. L. Markley, and R. H. Fillingame. 1998. Solution structure of the transmembrane H+-transporting subunit c of the F1F0 ATP synthase. *Biochemistry.* 37:8817–8824.

Hammes-Schiffer, S. 1996. Multiconfigurational molecular dynamics with quantum transitions: multiple proton transfer reactions. *J. Chem. Phys.* 105:2236–2246.

Hummer, G., J. C. Rasaiah, and J. P. Noworyta. 2001. Water conduction through the hydrophobic channel of a carbon nanotube. *Nature.* 414:188–190.

Hwang, J.-K., G. King, S. Creighton, and A. Warshel. 1988. Simulation of free energy relationships and dynamics of S_n2 reactions in aqueous solution. *J. Am. Chem. Soc.* 110:5297–5311.

Hwang, J.-K., and A. Warshel. 1996. How important are quantum mechanical nuclear motions in enzyme catalysis? *J. Am. Chem. Soc.* 118:11745–11751.

Jensen, M. Ø., E. Tajkhorshid, and K. Schulten. 2003. Electrostatic tuning of permeation and selectivity in aquaporin water channels. *Biophys. J.* 85:1–16.

Johnson, E. T., and W. W. Parson. 2002. Electrostatic interactions in an integral membrane protein. *Biochemistry.* 41:6483–6494.

Kannt, A., R. D. Lancaster, and H. Michel. 1998. The coupling of electron transfer and proton translocation: electrostatic calculations on *Paracoccus dentrificans* cytochrome c oxidase. *Biophys. J.* 74:708–721.

King, G., and A. Warshel. 1989. A surface-constrained all-atom solvent model for effective simulations of polar solutions. *J. Chem. Phys.* 91: 3647–3661.

Kitzing, E., and D. M. Soumpasis. 1996. Electrostatics of a simple membrane model using Green's functions formalism. *Biophys. J.* 71: 795–810.

Kong, Y., and G. Ma. 2001. Dynamic mechanisms of the membrane water channel aquaporin-1 (AQP1). *Proc. Natl. Acad. Sci. USA.* 98:14345–14349.

Kong, Y., and A. Warshel. 1995. Linear free energy relationships with quantum mechanical corrections: classical and quantum mechanical rate constants for hydride transfer between NAD^+ analogs in solutions. *J. Am. Chem. Soc.* 117:6234–6242.

Lancaster, C. R. D., H. Michel, and B. Honig. 1996. Calculated coupling of electron and proton transfer in the photosynthetic reaction center of *Rhodopseudomonas viridis*. *Biophys. J.* 70:2469–2492.

Law, R. J., and M. S. P. Sansom. 2002. Water transporters: how so fast yet so selective? *Curr. Biol.* 12:R250–R252.

Lee, F. S., Z. T. Chu, and A. Warshel. 1993. Microscopic and semimicroscopic calculations of electrostatic energies in proteins by the POLARIS and ENZYMIX programs. *J. Comp. Chem.* 14:161–185.

Lee, F. S., and A. Warshel. 1992. A local reaction field method for fast evaluation of long-range electrostatic interactions in molecular simulations. *J. Chem. Phys.* 97:3100–3107.

Luecke, H. 2000. Atomic resolution structures of bacteriorhodopsin photocycle intermediates: the role of discrete water molecules in the function of this light-driven ion pump. *Biochim. Biophys. Acta.* 1460:133–156.

Luecke, H., B. Schobert, H. T. Richter, J. P. Cartailler, and J. K. Lanyi. 1999. Structure of bacteriorhodopsin at 1.55 Å resolution. *J. Mol. Biol.* 291:899–911.

Marcus, R. A. 1964. Chemical and electrochemical electron transfer theory. *Annu. Rev. Phys. Chem.* 15:155–196.

Marrink, S. J., F. Jahnig, and H. J. Berendsen. 1996. Proton transport across transient single-file water pores in a lipid membrane studied by molecular dynamics simulations. *Biophys. J.* 71:632–647.

Mitchell, P. 1961. Coupling of phosphorylation to electron and hydrogen transfer by a chemi-osmotic type of mechanism. *Nature.* 191:144–148.

Murata, K., K. Mitsuoka, T. Hiral, T. Waltz, P. Agrel, J. B. Heymann, A. Engel, and Y. Fujlyoshi. 2000. Structural determinants of water permeation through aquaporin-1. *Nature.* 407:599–605.

Nagle, J. F., and M. Mille. 1981. Molecular models of proton pumps. *J. Chem. Phys.* 74:1367–1372.

Nagle, J. F., and H. J. Morowitz. 1978. Theory of hydrogen-bonded chains in bioenergetics. *Proc. Natl. Acad. Sci. USA.* 75:298–302.

Okamura, M. Y., and G. Feher. 1992. Proton transfer in reaction centers from photosynthetic bacteria. *Annu. Rev. Biochem.* 61:861–896.

Ostermeier, C., A. Harrenga, U. Ermler, and H. Michel. 1997. Structure at 2.7 A resolution of the *Paracoccus dentrificans* two-subunit cytochrome-c oxidase complexed with an antibody FV fragment. *Proc. Natl. Acad. Sci. USA.* 94:10547–10553.

Parsegian, A. 1969. Energy of an ion crossing a low dielectric membrane: solutions to four relevant electrostatic problems. *Nature.* 221:844–846.

Pomès, R., and B. Roux. 1998. Free energy profiles for H^+ conduction along hydrogen-bonded chains of water molecules. *Biophys. J.* 75:33–40.

Pomès, R., and B. Roux. 2002. Molecular mechanism of H^+ conduction in the single-file chain of the gramicidin channel. *Biophys. J.* 82:2304–2316.

Royant, A., K. Edman, T. Ursby, E. Pebay-Peyroula, E. M. Landau, and R. Neutze. 2000. Helix deformation is coupled to vectorial proton transport in the photocycle of bacteriorhodopsin. *Nature.* 406:645–648.

Sansom, M. S. P., and R. J. Law. 2001. Aquaporins—channels without ions. *Curr. Biol.* 11:R71–R73.

Sass, H. J., G. Buldt, R. Gessenich, D. Hehn, D. Neff, R. Schlesinger, J. Berendzen, and P. Ormos. 2000. Structural alterations for proton translocation in the *M* state of wild-type bacteriorhodopsin. *Nature.* 406:649–653.

Scheiner, S. 1981. Proton transfers in hydrogen-bonded systems. Cationic oligomers of water. *J. Am. Chem. Soc.* 103:315–320.

Schmitt, U. W., and G. A. Voth. 1998. Multistate empirical valence bond model for proton transport in water. *J. Phys. Chem. B.* 102:5547–5551.

Schutz, C. N., and A. Warshel. 2001. What are the dielectric ''constants'' of proteins and how to validate electrostatic models. *Prot. Struc. Func. Gen.* 44:400–417.

Schweins, T., and A. Warshel. 1996. Mechanistic analysis of the observed linear free energy relationships in p21 ras and related systems. *Biochemistry.* 35:14232–14243.

Sham, Y., I. Muegge, and A. Warshel. 1999. Simulating proton translocations in proteins: probing proton transfer pathways in the *Rhodobacter sphaeroides* reaction center. *Proteins.* 36:484–500.

Sham, Y. Y., Z. T. Chu, and A. Warshel. 1997. Consistent calculations of pK_as of ionizable residues in proteins: semi-microscopic and macroscopic approaches. *J. Phys. Chem. B.* 101:4458–4472.

Sham, Y. Y., I. Muegge, and A. Warshel. 1998. The effect of protein relaxation on charge-charge interactions and dielectric constants of proteins. *Biophys. J.* 74:1744–1753.

Strajbl, M., G. Hong, and A. Warshel. 2002. Ab-initio QM/MM simulation with proper sampling: ''first principle'' calculations of the free energy of the auto-dissociation of water in aqueous solution. *J. Phys. Chem. B.* 106:13333–13343.

Sui, H., B.-G. Han, J. K. Lee, P. Walian, and B. K. Jap. 2001. Structural basis of water-specific transport through the AQP1 water channel. *Nature.* 414:872–878.

Tajkhorshid, E., P. Nollert, M. Jensen, L. Miercke, R. M. Stroud, and K. Schulten. 2002. Control of the selectivity of the aquaporin water channel by global orientational tuning. *Science.* 296:525–530.

Villa, J., and A. Warshel. 2001. Energetics and dynamics of enzymatic reactions. *J. Phys. Chem. B.* 105:7887–7907.

Vuilleumier, R., and D. Borgis. 1998. An extended empirical valence bond model for describing proton transfer in $H^+(H_20)_n$ clusters and liquid water. *Chem. Phys. Lett.* 284:71–77.

Vuilleumier, R., and D. Borgis. 1999. Transport and spectroscopy of the hydrated proton: a molecular dynamics study. *J. Chem. Phys.* 111:4251–4266.

Warshel, A. 1979. Conversion of light energy to electrostatic energy in the proton pump of *Halobacterium halobium*. *Photochem. Photobiol.* 30:285–290.

Warshel, A. 1981. Energetics of light-induced charge separation across membranes. *Isr. J. Chem.* 21:341–347.

Warshel, A. 1982. Dynamics of reactions in polar solvents. semiclassical trajectory studies of electron-transfer and proton-transfer reactions. *J. Phys. Chem.* 86:2218–2224.

Warshel, A. 1984a. Dynamics of enzymatic reactions. *Proc. Natl. Acad. Sci. USA.* 81:444–448.

Warshel, A. 1984b. Simulating the energetics and dynamics of enzymatic reactions. *Pontificiae Academiae Scientiarum Scripta Varia.* 55(Specif. Biol. Interact.):59–81.

Warshel, A. 1986. Correlation between structure and efficiency of light-induced proton pumps. *In* Methods in Enzymology. L. Packer, editor. Academic Press, London, UK. 578–587.

Warshel, A. 1991. Computer Modeling of Chemical Reactions in Enzymes and Solutions. John Wiley & Sons, New York.

Warshel, A. 2002. Molecular dynamics simulations of biological reactions. *Acc. Chem. Res.* 35:385–395.

Warshel, A. 2003. Computer simulations of enzyme catalysis: methods, progress, and insights. *Annu. Rev. Biophys. Biomol. Struct.* 32:425–443.

Warshel, A., J. Aqvist, and S. Creighton. 1989. Enzymes work by solvation substitution rather than by desolvation. *Proc. Natl. Acad. Sci. USA.* 86:5820–5824.

Warshel, A., and M. Levitt. 1976. Theoretical studies of enzymic reactions: dielectric, electrostatic and steric stabilization of the carbonium ion in the reaction of lysozyme. *J. Mol. Biol.* 103:227–249.

Warshel, A., and S. T. Russell. 1984. Calculations of electrostatic interactions in biological systems and in solutions. *Q. Rev. Biophys.* 17: 283–421.

Warshel, A., S. T. Russell, and A. K. Churg. 1984. Macroscopic models for studies of electrostatic interactions in proteins: limitations and applicability. *Proc. Natl. Acad. Sci. USA.* 81:4785–4789.

Warshel, A., and D. W. Schlosser. 1981. Electrostatic control of the efficiency of light-induced electron transfer across membranes. *Proc. Natl. Acad. Sci. USA.* 78:5564–5568.

Warshel, A., T. Schweins, and M. Fothergill. 1994. Linear free energy relationships in enzymes. theoretical analysis of the reaction of tyrosyl-tRNA synthetase. *J. Am. Chem. Soc.* 116:8437–8442.

Warshel, A., and R. M. Weiss. 1980. An empirical valence bond approach for comparing reactions in solutions and in enzymes. *J. Am. Chem. Soc.* 102:6218–6226.

Wikstrom, M. 1998. Proton translocation by bacteriorhodopsin and heme-copper oxidases. *Curr. Op. Struct. Biol.* 8:480–488.

Wu, Y., and G. A. Voth. 2003. A computer simulation study of the hydrated proton in a synthetic proton channel. *Biophys. J.* 85:864–875.

Yoshikawa, S., K. Shinzawa-Itoh, R. Nakashima, R. Yaono, E. Yamashita, N. Inoue, M. Yao, M. J. Fei, C. P. Libeu, T. Mizushima, H. Yamaguchi, T. Tomizaki, and T. Tsukihara. 1998. Redox-coupled crystal structural changes in bovine heart cytochrome c oxidase. *Science.* 280:1723–1729.

Zeuthen, T. 2001. How water molecules pass through aquaporins. *Trends Biochem. Sci.* 26:77–78.

Zundel, G., and J. Frish. 1986. Chapter 2. *In* The Chemical Physics of Solvation, Vol. 2. Elsevier, Amsterdam, The Netherlands.